Calculation of the Viscous Resistance of Bodies of Revolution

A. Nakayama* and V. C. Patel†
Iowa Institute of Hydraulic Research, University of Iowa, Iowa City, Iowa

The flow in the tail region of a body of revolution is a complex one since there the boundary layer often grows to a thickness many times the local radius of the body and there results a strong interaction between the boundary layer and the external potential flow. The influence of making simplifying assumptions concerning the flow in this region in conventional drag-calculation methods is discussed and assessed by incorporating a method which takes into account the effects of the thick axisymmetric boundary layer near the tail in an approximate manner. It is shown that this modification leads to a drag-calculation method which gives consistently accurate prediction of the viscous resistance of a wide variety of bodies of revolution.

Nomenclature

C_D = drag coefficient [$= D/(1/2)\rho U_\infty{}^2 V^{2/3}$ unless otherwise stated]
C_p = pressure coefficient [$(p - p\ )/(1/2)\rho U_\infty{}^2$]
C_P = prismatic coefficient ($= 4V/\pi d^2 L$)
d = maximum diameter of a body
D = viscous drag
H = shape factor ($= \delta_1/\delta_2$)
L = total length of a body
m = position of $r_{\max}$ ($= X_m/L$)
p = pressure
p = undisturbed freestream pressure
r = distance to the axis of a body of revolution
r_o = local radius of a body of revolution
$r_{\max}$ = maximum local radius of a body of revolution
r_n = nose radius of curvature
r_t = tail radius of curvature
R_e = Reynolds number ($= U\ \ L/\nu$)
R_n = nondimensional nose radius ($= r_n L/d^2$)
R_t = nondimensional tail radius ($= r_t L/d^2$)
R_x = Reynolds number based on x ($= U_e x/\nu$)
R_δ = Reynolds number based on δ ($= U_e\delta/\nu$)
R_θ = Reynolds number based on δ_2 ($= U_e\delta_2/\nu$)
S = characteristic area of a body
u' = rms value of the velocity fluctuations in the freestream
U = velocity component in the x-direction
U_e = velocity component in the x-direction at the edge of the boundary layer
U_∞ = undisturbed freestream velocity
V = volume of a body
x = distance along the surface of a body from the nose
X = axial distance from the nose
X_m = axial distance to the point of maximum radius
X_{tr} = axial distance to the transition from the laminar to turbulent boundary layer
y = distance to a point normal to the surface
δ = boundary-layer thickness
δ_1 = displacement thickness
δ_2 = momentum thickness
Δ_1 = displacement area
Δ_2 = momentum area
λ = pressure gradient parameter $\left(= \dfrac{\delta_2{}^2}{\nu}\dfrac{dU_e}{dx}\right)$
Λ = pressure gradient parameter $\left(= \dfrac{\delta^2}{\nu}\dfrac{dU_e}{dx}\right)$
ν = kinematic viscosity of a fluid
ρ = density of a fluid

Received November 30, 1973; revision received May 17, 1974. This paper is based upon research conducted under the General Hydromechanics Research Program of the Naval Ship Systems Command, technically administered by the Naval Ship Research and Development Center, under Contract N00014-68-A-0196-0002.
Index category: Hydrodynamics.
*Research Assistant.
†Associate Professor and Research Engineer.

I. Introduction

THERE has always been a certain amount of ambiguity in the calculation of the viscous resistance of a body of revolution stemming from the treatment of the flow in the region near the tail of the body. In order to calculate the resistance in the absence of separation, either by the application of the well-known Squire-Young method or by the continuation of a boundary-layer type calculation through the near wake to predict the momentum deficit in the far wake, it is necessary to know the characteristics of the boundary layer at the tail and also the velocity just outside the boundary layer at this point. As pointed out recently by Patel, Nakayama, and Damian,[1] the flow in the tail region of the body (the rear 10–15% of the body length, say) requires special attention for two reasons: a) the usual thin boundary-layer approximations cease to apply in this region since the boundary layer often grows to a thickness many times the local radius of the body, and b) there exists substantial interaction between the thick boundary layer and the potential flow outside it, so that potential-flow theory, by itself, predicts neither the pressure distribution on the surface nor the freestream velocity distribution which the boundary layer sees. For the calculation of the boundary-layer development in this region, the viscous correction for the pressure distribution must be considered. In previous methods for the calculation of drag, such as those of Granville,[2] Cebeci, Mosinskis, and Smith,[3] and Parsons and Goodson,[4] these effects have been taken into account by continuing the boundary-layer calculation into the tail region using some pressure distribution obtained by arbitrarily extrapolating the potential-flow pressure distribution from further upstream. However, only the usual thin boundary-layer calculation methods have been used thus far to determine the required parameters of the boundary layer at the tail. The influence of these assumptions on the final predition of the resistance of bodies of revolution remains undetermined. The complex nature of the flow in the tail region has been discussed recently by Patel[5] and it appears that a satisfactory solution of the problem must await further investigations of the influence of strong transverse curvature on turbulent boundary layers and also the development of procedures for the calculation of the interaction between the boundary layer and the potential flow. As a first step towards assessing the importance of the flow in the tail region, however, an integral method proposed recently by Patel[6] for the calculation of THICK, axisymmetric, turbulent boundary layers has been incorporated in the more or less conventional drag calculation scheme. This paper describes the results of that study.

A computer program has been developed for the calculation of the viscous resistance of a streamlined body of revolution placed axially in a uniform, incompressible stream. When the dimensions of the body and the Reynolds number are specified, the program first finds the potential-flow pressure distribution on the body surface. The laminar boundary layer over the nose portion of the body is then calculated. This is terminated at the point where transition to turbulent flow takes place. The location of the transition point may be prescribed a priori, or it may be determined by the use of any one of the transition criteria available in the literature. Some of the well-known criteria have been employed in this work in order to evaluate their relative merits and also to study the influence of the position of transition on the resistance of the body. Beyond transition, the development of the turbulent boundary layer is calculated using the method of Patel mentioned earlier. Finally, the resistance of the body is calculated using the Squire-Young method in conjunction with the shape parameter and the momentum thickness predicted in the tail region. Herein lies another departure from procedures used previously. In addition to using an extrapolated pressure distribution in the tail region, the boundary-layer calculations are also performed using the potential-flow pressure distribution. The difficulties associated with this latter procedure were, however, avoided by employing a Squire-Young type formula after each step in the boundary-layer calculation over the last 10% of the body, to determine the variation of the drag coefficient with length along it. The successive values of "drag coefficient" obtained in this manner were found to increase up to some point and decrease thereafter as the boundary-layer calculation approached the tail of the body. The required drag coefficient of the body was simply taken to be the maximum value. Comparisons made with the values obtained by using the experimentally measured and extrapolated pressure distributions in place of the potential-flow pressure distribution suggested that this procedure yields acceptable results.

The resistance coefficients calculated by the present method have been compared with available experimental data for a wide variety of bodies of revolution. These comparisons show that the resistance of bodies of revolution can be predicted with considerable accuracy provided the exact location of the transition point is known or can be found.

II. Details of the Method of Calculation

The various elements which constitute the present drag-calculation scheme were outlined in the Introduction. With the exception of the turbulent boundary-layer calculation method and the application of a Squire-Young type formula, the calculation procedures used here are quite well-known. We shall therefore describe these briefly in Secs. II-A to II-E, elaborating only upon those aspects which are new.

A. Potential-Flow Calculation

There are, of course, a number of methods available for the solution of the potential flow on an axisymmetric body placed in a uniform axial stream. Among these, the method developed by Landweber[7] in which the problem is reduced to the solution of a Fredholm integral equation of the first kind, appeared to be the best suited to the present study since it is relatively simple to use. The general derivation of the integral equation and a suitable iterative numerical procedure for its solution have been described in detail by Landweber. This procedure was utilized, with some minor modification, in the present study. Although gauss quadrature of order 16 (i.e., the use of 16 coordinate points to specify the shape of the body) originally recommended gave acceptable results, the order was changed to 24 so that a simple interpolation formula could be used with sufficient accuracy to find the required pressure gradients in the boundary-layer calculations. A convergence criterion was also incorporated in order to stop the iteration procedure when a desired level of accuracy was reached. During the course of this work it was observed that, to obtain reliable and smooth pressure distributions, the coordinates of the body had to be specified with considerable precision.

The pressure distributions calculated using this method are compared with four sets of experimental data in Figs. 1a–1d. The body shapes are also shown in these figures. The pressure coefficient C_P is defined as follows:

$$C_p = (p - p_\infty)/1/2\rho U_\infty^2 \tag{1}$$

where p is pressure at any point on the body, U is velocity, ρ is density and the subscript ∞ refers to values in the undisturbed stream. It will be seen that the agreement between experiment and potential-flow theory is satisfactory over most of the body surface in the first three cases shown. In the last case, namely that of Cornish and Boatwright,[8] the lack of close agreement may be because these measurements were made on a full-scale airship which was not truly axisymmetric owing to the presence of control surfaces. The departure of the experimental pressure distribution from potential-flow theory in the tail region, commented upon earlier and attributed to the strong interaction between the boundary layer and the external flow, is well illustrated by the experiments of Lyon[9] shown in Figs. 1b and 1c.

B. Laminar Boundary-Layer Development.

For the calculation of the laminar boundary layer over the nose portion of the body, the method of Thwaites,[10] as modified by Rott and Crabtree[11] for axisymmetric flow, was employed. In this method, the momentum-integral equation is reduced to a simple quadrature formula of the form

$$\delta_2^2 = 0.47\nu r_o^{-2} U_e^{-6} \int_0^x r_o^2 U_e^5 dx \tag{2}$$

where δ_2 is the momentum thickness of the boundary layer defined in the manner appropriate for axisymmetric flow [see Eq. (6)], ν is kinematic viscosity, x is the distance measured along the body surface from the nose, $r_o(x)$ is the radius distribution of the body, and $U_e(x)$ is the freestream velocity outside the boundary layer obtained from the potential flow pressure distribution calculated previously, viz.,

$$U_e/U_\infty = (1 - C_p)^{1/2} \tag{3}$$

Note that the small but finite value of the momentum thickness at the nose of the body ($x = 0$) is ignored.

The momentum thickness calculated from Eq. (2) was used in the prediction of transition to turbulent flow in the manner described in Sec. II-C. For transition criteria which require information concerning laminar boundary-layer parameters other than the momentum thickness, however, such parameters were found from the singly-infinite family of velocity profiles of Pohlhausen and the calculated momentum thickness.

C. Prediction of Transition

Numerous empirical or semi-empirical criteria have been proposed in the past for the prediction of transition from laminar to turbulent flow. From these, the criteria

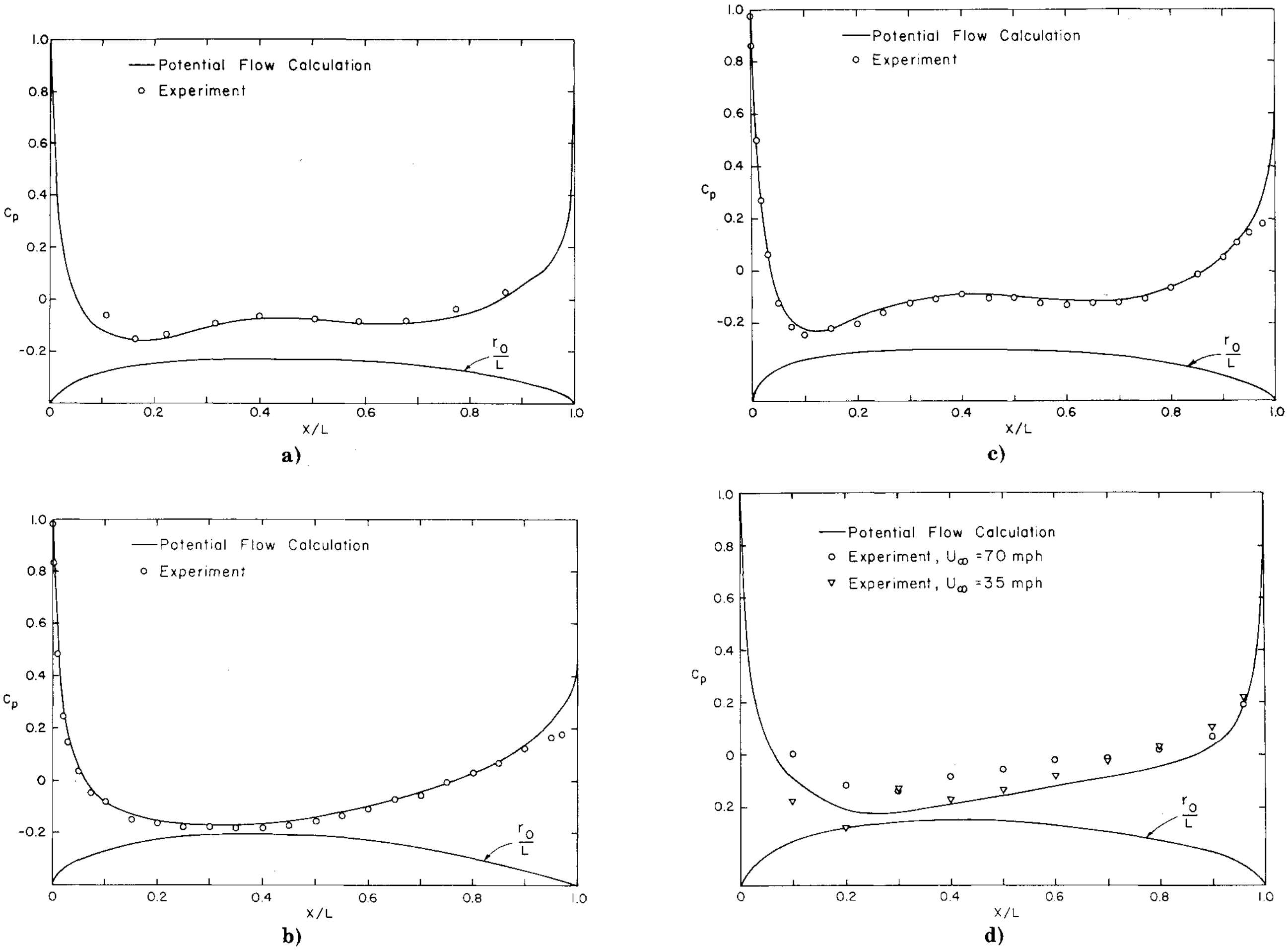

Fig. 1 Comparison between experimental and potential flow pressure distributions. a) Model of Airship Akron, Freeman. b) Model A of Lyon. c) Model B of Lyon. d) U.S. Navy Airship, Cornish and Boatwright.

due to Michel;[12] Granville;[2] Crabtree;[13] van Ingen;[14] van Driest and Blumer;[15] Jaffe, Okamura, and Smith;[6] and Hall and Gibbings[17] were examined during the course of this work but, for reasons of simplicity, only the four listed in Table 1 were finally incorporated in the drag calculation scheme. The parameters which are required for the calculation of the transition point according to these criteria are also listed. Here, u' is the rms value of the velocity fluctuations in the freestream; R_θ, R_δ, and R_x are local Reynolds numbers defined by

$$R_\theta = \frac{U_e \delta_2}{\nu},\ R_\delta = \frac{U_e \delta}{\nu},\ R_x = \frac{U_e x}{\nu} \tag{4}$$

and Λ and λ are pressure-gradient parameters defined by

$$\Lambda = \frac{\delta^2}{\nu}\frac{dU_e}{dx},\ \lambda = \frac{\delta_2{}^2}{\nu}\frac{dU_e}{dx} \tag{5}$$

where δ is the physical thickness of the boundary layer. The parameters ΔR_θ and $\bar{\Lambda}$ appearing in the method of Granville are, respectively, the change in R_θ and the average value of Λ between the point of neutral stability as indicated by stability theory and the point of self-excited transition.

In the method of Van Driest and Blumer, the value of R at transition is related to Λ and u'/U_e via a simple equation. In the other three cases, the value of R_θ at transition is obtained from the other parameters by the use of correlation curves presented graphically by the originators. These curves were read into the computer in the form of tables and were used in conjunction with suitable interpolation formulas.

The four criteria listed previously were used, in turn, to determine the transition point. At this point the calculation of the laminar boundary layer was terminated and the turbulent boundary-layer calculations described in Sec. II-D were initiated. Calculations were also performed using the experimentally observed transition point when this was known.

D. Turbulent Boundary-Layer Calculation

In order to calculate the development of the turbulent boundary layer, values have to be assigned to the parameters R_θ and H immediately following transition. The value of R_θ presents no problem in the case of natural transition since it remains constant across transition. The value of H corresponding to this R_θ and the local pressure gradient was then inferred from the relations between the various parameters given by Nash[18] for equilibrium boundary layers and the skin-friction formula of Thompson.[19] It should be pointed out here that in cases where transition is promoted by artificial finite disturbances, such as boundary-layer trips, boundary-layer calculations should be performed after taking into account the additional momentum thickness due to the transition devices or using the experimental values of H and R_θ downstream of transition. This procedure was not, however, necessary in the cases treated here.

The turbulent boundary-layer calculation method used here is described in detail by Patel.[6] This method is capable of predicting the development of thin as well as thick

Table 1 Transition criteria and parameters

Transition Criterion	Parameters
Michel[12]	R_θ, R_x
Granville[2]	R_θ, Λ, ΔR_θ, $\bar{\Lambda}$, u'/U_∞
Crabtree[13]	R_θ, λ
Van Driest and Blumer[15]	R_δ, Λ, u'/U_e

axisymmetric boundary layers, and for thin boundary layers it reduces identically to the extension of the method of Head[20] proposed for axisymmetric flow by Shanebrook and Sumner.[21] The thick boundary-layer effects over the tail of the body are taken into account in an approximate manner by the use of a) the freestream velocity distribution implies by either the potential-flow or the extrapolated pressure distribution on the surface rather than the actual freestream velocity distribution that exists as a result of the interaction between the boundary layer and the potential flow, and b) generalized forms of Head's entrainment and shape-parameter relations. Some calculations were also performed using the Shanebrook and Sumner form of Head's method into the tail region in order to ascertain the influence of taking the thick boundary-layer effects into account.

E. Prediction of Drag Coefficient

The turbulent boundary-layer calculation method described above predicts, among other things, the growth of the displacement and momentum thicknesses defined in a manner appropriate to axisymmetric boundary layers, viz.,

$$\delta_1 = \int_0^\delta \left(1 - \frac{U}{U_e}\right)\frac{r}{r_o}dy, \quad \delta_2 = \int_0^\delta \frac{U}{U_e}\left(1 - \frac{U}{U_e}\right)\frac{r}{r_o}dy \tag{6}$$

where y is the distance measured normal to the surface, r is the distance from the axis of the body, and U is the velocity distribution in the boundary layer. Since r_o becomes zero at the tail of the body, δ_1 and δ_2 become infinite there. However, the values of the displacement and momentum areas, defined as

$$\Delta_1 = 2\pi r_o \delta_1 \, , \quad \Delta_2 = 2\pi r_o \delta_2 \tag{7}$$

can be found, and these remain finite at the tail. For a body of revolution, the Squire-Young drag formula, as given by Young,[22] may be written

$$\left.\begin{aligned} C_D &= \frac{2\Delta_2}{S}\left[\frac{U_e}{U_\infty}\right]^a \\ a &= (1/2)(H + 5) \end{aligned}\right\} \tag{8}$$

where

$$C_D \equiv \frac{D}{1/2\rho U_\infty{}^2 S} \tag{9}$$

is the drag coefficient, D is the drag force on the body, and S is a characteristic area of the body (e.g., the maximum cross-section area or the total surface area). All quantities in Eq. (8) are to be evaluated at the tail of the body. A formula somewhat similar to Eq. (8) has also been suggested by Granville[2]:

$$\left.\begin{aligned} C_D &= \frac{2\Delta_2}{S}\left(\frac{U_e}{U_\infty}\right)^b \\ b &= (1/8)[7(H + 2) + 3] \end{aligned}\right\} \tag{10}$$

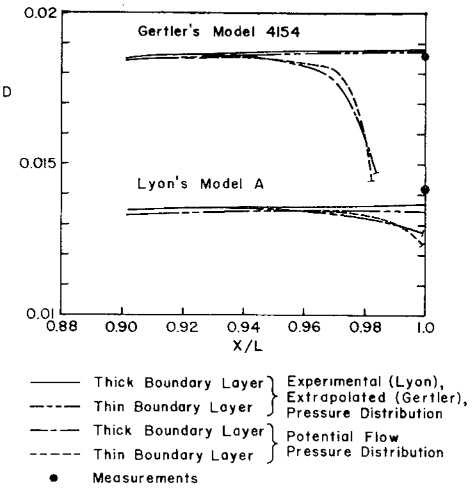

Fig. 2 Determination of drag coefficient by the use of Granville's formula after each step in the boundary-layer calculation.

This latter formula was used in the drag calculations described below.

Owing to the interaction between the thick boundary layer and the external flow, and the observation that conventional thin boundary-layer calculation procedures cannot be used in the tail region, it is not possible to evaluate accurately the boundary-layer parameters Δ_1 and Δ_2, and the freestream velocity U_e, at the tail, occurring in Eqs. (8) and (10). Even the extrapolated or experimental pressure distributions on the surface of the body do not give the magnitude of U_e, the velocity at the edge of the boundary layer. Instead of extrapolating potential-flow pressure distributions into the tail region as suggested in previous studies, an alternative procedure, in which the boundary-layer parameters, based on the potential-flow pressure distribution, are extrapolated, can be used. For the calculation of the drag coefficient, it is in fact easier to use the drag formula, Eq. (10), after each step in the boundary-layer calculation, and study the behavior of the successive values of C_d. Figure 2 shows the results of such calculations for one of the models tested by Lyon,[9] and one of the series of bodies tested by Gertler.[23] Also shown in the figure are the values of C_D predicted in this manner using the experimental pressure distribution in the case of Lyon, and the extrapolated potention-flow pressure distribution suggested by Cebeci et al.[3] for the case of Gertler. It will be seen that the use of the experimental or extrapolated pressure distributions lead to an unambiguous value for the drag coefficient. On the other hand, the successive values of C_D, obtained by using the potential-flow pressure distribution, reach a maximum somewhat ahead of the tail and then decrease as the tail is approached. The breaks in the C_D curves indicate that the boundary-layer calculation predicted separation at that point. The maximum value of C_D is then taken to be the drag coefficient of the body. This implies that the drag formula, Eqs. (10), which attempt to describe the flow in the wake of the body, is now assumed to represent a solution of the flow downstream of the point where C_D reaches a maximum value. The major justification for the proposed procedure lies in the fact that it represents an extrapolation of the boundary-layer parameters rather than the potential-flow pressure distribution. It will be seen in Sec. III that this procedure leads to acceptable results for the drag coefficient even when the boundary-layer calculations indicate separation some distance ahead of the tail.

In order to assess the influence of using a thin boundary-layer method up to the tail, the preceding calculations were repeated using the method of Shanebrook and Sumner[21] in place of the thick boundary-layer method of

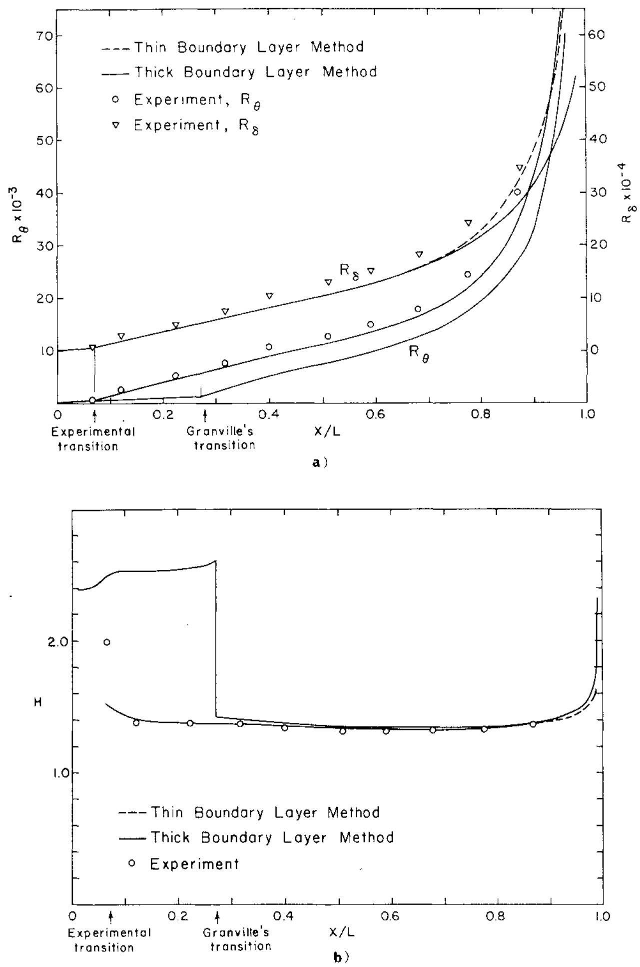

Fig. 3 Boundary-layer development: Airship Akron, Freeman. a) Experimental. b) Calculated.

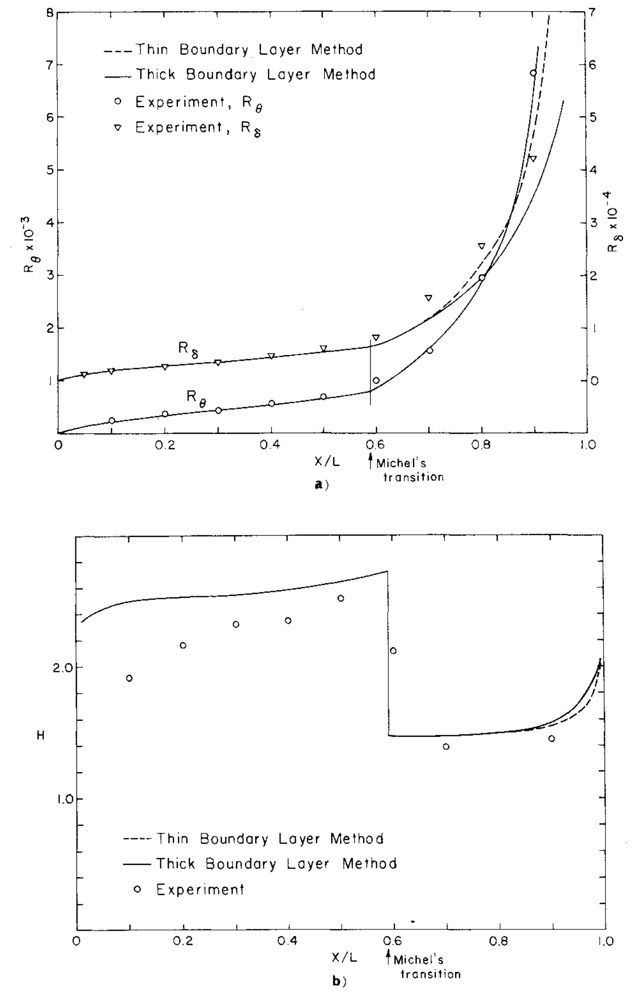

Fig. 4 Boundary-layer development: Model A, Lyon. a) Experimental. b) Calculated.

Patel.[6] The results of these calculations are also shown in Fig. 2. It is remarkable that the inclusion of the thick boundary-layer method makes no significant improvement in the prediction of the drag coefficient, although, as remarked later on, the behavior of the boundary layer predicted by the thick and the thin boundary-layer methods is substantially different in the tail region. While the thick boundary-layer method predicts values of H and Δ_2, which are higher than those predicted by the thin boundary-layer method, Eqs. (10) remain insensitive to these differences. The retention of the thick boundary-layer method is however recommended, not only because it is safer to do so, but also because it would be more appropriate if the drag formula is discarded in favor of drag-prediction methods based on the continuation of boundary-layer-type calculations into the near and far wake.

III. Results and Discussion

Before describing the results of the over-all drag calculations it is useful to examine, very briefly, the perfor-

Table 2 Experimental and calculated drag coefficients using various transition criteria

	Measurements			Method of transition prediction									
				Experimental transition		Michel's method		Granville's method		Van Driest and Blumer's method		Crabtree's method	
	$R_e = \frac{U_\infty L}{\nu}$	X_{tr}/L	C_D	X_{tr}/L	C_D	X_{tr}/L	C_D	X_{tr}/L	C_D	X_{tr}/L	C_D	X_{tr}/L	C_D
Freeman's Akron Model	1.73×10^7	0.06 ~ 0.07	0.0190 (wooden) 0.0219 (metal)	0.070	0.0198	0.552	0.0100	0.272	0.0161	0.252	0.0165	0.262	0.0163
Lyon's Model A	2.04×10^6	0.5 ~ 0.7	0.0142	0.60	0.0132	0.592	0.0135	0.632	0.0123	0.632	0.0123	0.612	0.0129
Lyon's Model B	2.04×10^6	0.25 ~ 0.35	0.0236	0.332	0.0218	0.652	0.0132	0.722	0.0113	0.732	0.0110	0.722	0.0113
U. S. Navy ZS2G-1	1.77×10^8	Not known	0.0125	...	...	Not applicable		0.160	0.0113	0.06	0.0122	0.132	0.0116

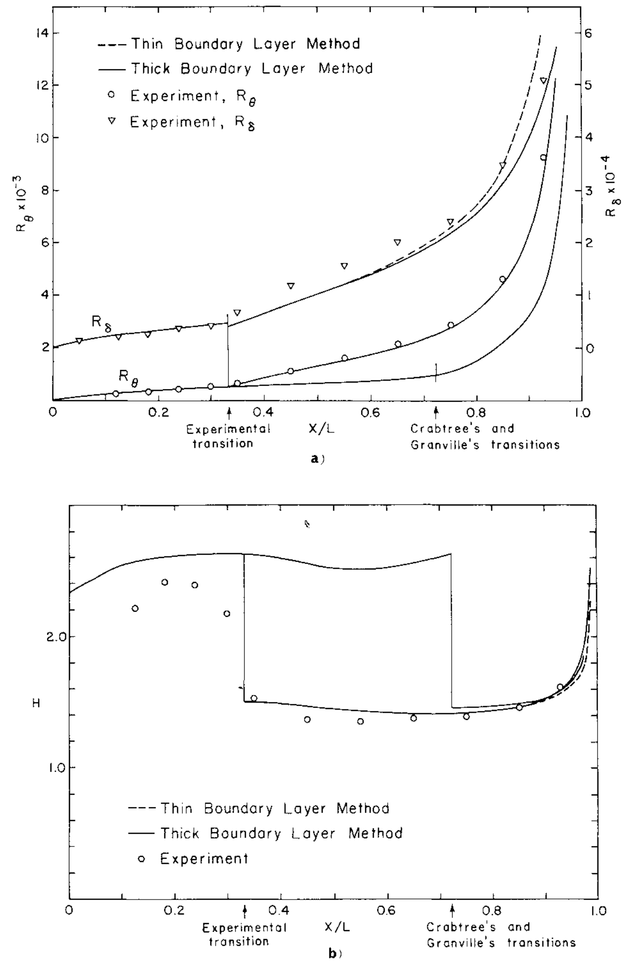

Fig. 5 Boundary-layer development: Model B, Lyon. a) Experimental. b) Calculated.

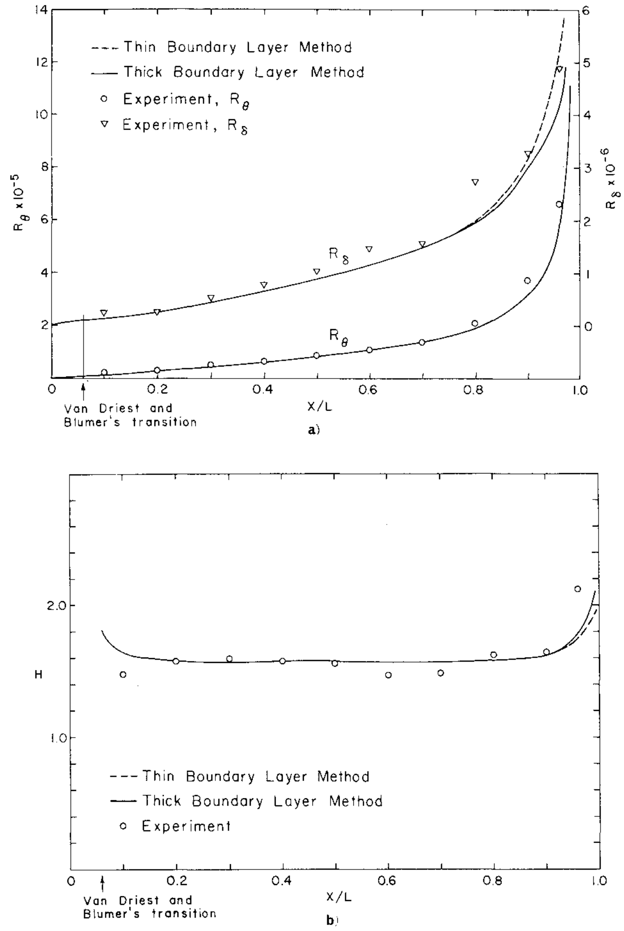

Fig. 6 Boundary-layer development: U.S. Navy Airship, Cornish and Boatwright. a) Experimental. b) Calculated.

mance of the various components of the complete drag-calculation procedure. From the comparisons shown in Fig. 1 and discussed in Sec. II-A it was concluded that the method of Landweber gives satisfactory prediction of the potential-flow pressure distribution. To assess the accuracy of the boundary-layer calculations and the various transition criteria employed here, comparisons have been made with the experimental data from the four bodies of revolution considered earlier, namely the Airship Akron model of Freeman,[24,25] Models A and B of Lyon,[9] and the U.S. Navy ZS2G-1 Airship tested by Cornish and Boatwright.[8]

From the transition results summarized in Table 2 it will be seen that no single criterion predicts the experimental transition point with desired accuracy. The criteria of Granville and of van Driest and Blumer, predict transition correctly in two out of the three cases where transition was observed experimentally, while the methods of Michel and Crabtree give agreement with only one case. In view of this, the boundary-layer calculations performed using only the experimentally observed transition point and one other transition criterion are shown in Figs. 3–6. Also shown in these figures are the results of the calculations in which the thick turbulent boundary-layer method of Shanebrook and Sumner.[21] The calculations shown in Figs. 3–5 employed the potential-flow pressure distribution, but because of the disagreement between the experimental and the pressure distributions on the U.S. Navy Airship, attributed earlier to a lack of axial symmetry, the calculations in Fig. 6 were performed using the pressure distribution measured at the larger of the two Reynolds numbers.

The comparisons between the calculations and the experimental data suggest that the development of the laminar and the turbulent boundary layers is predicted satisfactorily, at least in the range covered by the measurements, provided the point of transition is either known or predicted accurately. It will be noticed that the results of the thick and the thin turbulent boundary-layer calculation methods differ appreciably (particularly with regard to the boundary-layer thickness and the shape parameter) in a small region near the tail of the bodies; but because of the lack of data in this region for the cases considered here, it is not possible to verify directly the conclusion of Patel,[6] based on other more detailed experimental data, that the thick boundary-layer method represents a considerable improvement over the thin boundary-layer method of Shanebrook and Sumner. The use of the potential-flow pressure distribution also implies that the present calculations will not be as satisfactory in detail as those made by Patel using the experimental pressure distributions.

The drag coefficients (based on $S = V^{2/3}$, where V is the volume of the body), for the four bodies of revolution, calculated using the different transition criteria and the thick boundary-layer calculation method are compared with the experimental values in Table 1. The values of C_D obtained by using the thin boundary-layer method were found to be within 1% of the tabulated values. It will be seen that the most consistent results are obtained when the location of the transition point coincides with the position observed experimentally.

Gertler[23] has reported the results of deep-submergence resistance tests on a large number of bodies of revolution, known as the Series 58 bodies, which were generated by systematically varying the fineness ratio, the prismatic coefficient, and the nose and tail radii (Landweber and Gertler[26]). These tests were performed over a range of

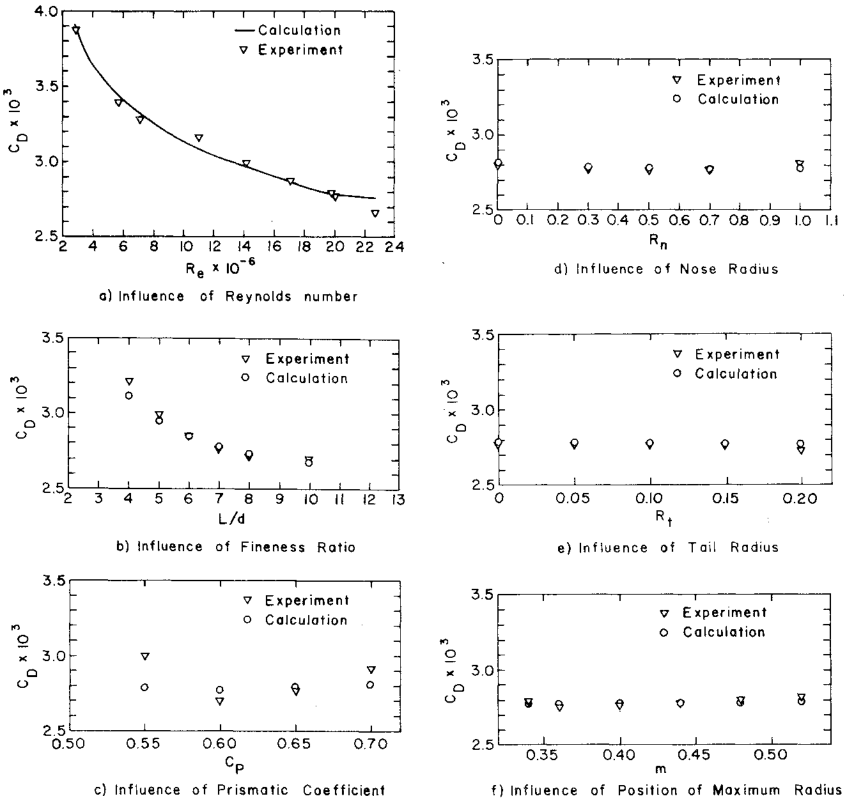

Fig. 7 Drag coefficients $[C_D = D/(\frac{1}{2}\rho U^2 S)]$ of the Series 58 bodies of Gertler.

Table 3 Experimental and calculated drag coefficients (based on the wetted surface area) for the Series 58 bodies of revolution

Model	Position of r_{max} $m \equiv \frac{X_m}{L}$	Nose radius $R_n \equiv \frac{r_n L}{d^2}$	Tail radius $R_t \equiv \frac{r_t L}{d^2}$	Prismatic coefficient $C_P \equiv \frac{4V}{\pi d^2 L}$	Fineness ratio L/d	Reynolds No. Re	Experimental $C_D \times 10^3$	Calculated $C_D \times 10^3$
4154	0.40	0.50	0.10	0.65	4.0	20.0	3.21	3.114
4155	0.40	0.50	0.10	0.65	5.0	20.0	2.99	2.984
4156	0.40	0.50	0.10	0.65	6.0	20.0	2.85	2.846
4157	0.40	0.50	0.10	0.65	7.0	2.85	3.87	3.905
4157	0.40	0.50	0.10	0.65	7.0	5.70	3.39	3.445
4157	0.40	0.50	0.10	0.65	7.0	7.10	3.27	3.318
4157	0.40	0.50	0.10	0.65	7.0	11.00	3.16	3.088
4157	0.40	0.50	0.10	0.65	7.0	14.20	2.99	2.966
4157	0.40	0.50	0.10	0.65	7.0	17.10	2.87	2.883
4157	0.40	0.50	0.10	0.65	7.0	19.80	2.79	2.818
4157	0.40	0.50	0.10	0.65	7.0	20.00	2.76	2.780
4157	0.40	0.50	0.10	0.65	7.0	22.70	2.66	2.763
4158	0.40	0.50	0.10	0.65	8.0	20.0	2.72	2.733
4159	0.40	0.50	0.10	0.65	10.0	20.0	2.70	2.674
4160	0.36	0.50	0.10	0.65	7.0	20.0	2.75	2.779
4161	0.44	0.50	0.10	0.65	7.0	20.0	2.78	2.781
4162	0.48	0.50	0.10	0.65	7.0	20.0	2.80	2.784
4163	0.52	0.50	0.10	0.65	7.0	20.0	2.82	2.788
4164	0.40	0.50	0.10	0.55	7.0	20.0	3.00	2.785
4165	0.40	0.50	0.10	0.60	7.0	20.0	2.70	2.775
4166	0.40	0.50	0.10	0.70	7.0	20.0	2.91	2.801
4167	0.40	0.00	0.10	0.65	7.0	20.0	2.79	2.819
4168	0.40	0.30	0.10	0.65	7.0	20.0	2.77	2.791
4169	0.40	0.70	0.10	0.65	7.0	20.0	2.77	2.773
4170	0.40	1.00	0.10	0.65	7.0	20.0	2.81	2.769
4171	0.40	0.50	0.00	0.65	7.0	20.0	2.76	2.789
4172	0.40	0.50	0.05	0.65	7.0	20.0	2.76	2.783
4173	0.40	0.50	0.15	0.65	7.0	20.0	2.76	2.778
4174	0.40	0.50	0.20	0.65	7.0	20.0	2.73	2.776
4175	0.40	0.50	0.10	0.60	5.0	20.0	2.95	2.933
4176	0.40	0.50	0.10	0.55	5.0	20.0	3.04	2.956
4177	0.34	0.50	0.10	0.65	7.0	20.0	2.79	2.780

Reynolds numbers but the position of transition was fixed in all cases at $X/L = 0.05$ by means of sand-paper strips. The present procedure, using the thick turbulent boundary-layer method, was applied to calculate the drag coefficient of a representative number of these bodies. The results of the calculations are compared with the experimental data in Table 2 and shown in Figs. 7a–7f. Note that here the drag coefficient is based on the total surface area. It will be seen that the present method again predicts the drag coefficient with acceptable accuracy.

IV. Conclusions

The drag calculation method proposed and verified here is a more or less conventional one except for the treatment of the flow in the tail region of the body of revolution. Rather surprisingly, the inclusion of the thick boundary-layer method in place of the thin boundary-layer method does not make a significant improvement in the drag prediction, although the boundary-layer characteristics in the tail region predicted by the two methods are grossly different. The drag calculation procedure, however, remains an approximate one for two reasons: 1) the potential-flow pressure distribution is used although this is not obtained in reality because of the interaction between the thick boundary layer and the external flow, and 2) the drag formula relating the drag coefficient to the boundary-layer parameters at the tail is, at best, a crude representation of the flow in the near and the far wake of the body. The fact that the present method gives a consistently accurate prediction of the drag for a wide variety of bodies of revolution does not, however, imply that the flow in the tail region of the body is unimportant. On the contrary, it indicates that the drag formula suggested by Squire and Young, and Granville, which contains information concerning the pressure distribution, and the boundary-layer parameters in the tail region, are in such a form that, by regarding the flow in the tail region as a part of the wake, they lead to a mutual cancellation of errors. The very fact that these formulas have stood the test of time vindicates this conclusion.

A more satisfactory procedure for the calculation of the drag of bodies of revolution can be developed by taking the flow in the tail region into account in a more direct and realistic manner. As pointed out by Patel,[5] this will involve the following steps: 1) calculation of the thick boundary layer right up to the tail using the potential-flow pressure distribution on the body as a first approximation; 2) continuation of a boundary-layer type calculation through the near wake into the far wake; 3) calculation of the pressure, or velocity distribution at the edge of the boundary layer and the wake by the application of potential-flow theory to the resulting semi-infinite domain; 4) evaluation of the pressure field between the body and the edge of the boundary layer and the wake from momentum considerations in the direction normal to the body surface; 5) a re-calculation of the boundary layer and the wake using this pressure field; and 6) iteration of the entire set of calculations until convergence is obtained. The drag on the body can then be found from the velocity and pressure variations across the boundary layer at the tail. The feasibility of such a procedure has not, however, been demonstrated conclusively so far. Apart from the convergence of such a scheme, major problems which may be encountered concern the development of methods which can calculate the near wake and the thick boundary layer across which there is a significant variation of static pressure. In the absence of such a refined drag calculation procedure, however, methods based on Squire-Young-type drag formula, such as the present one, can be used with a fair degree of confidence.

References

[1]Patel, V. C., Nakayama, A., and Damian, R., "An Experimental Study of the Thick Turbulent Boundary Layer Near the Tail of a Body of Revolution," Journal of Fluid Mechanics, Vol. 63, Pt. 2, April 1974, pp. 345–367.

[2]Granville, P. S., "The Calculation of Viscous Drag of Bodies of Revolution," Rept. 849, 1953, David Taylor Model Basin, Washington, D.C.

[3]Cebeci, T., Mosinskis, G. J., and Smith, A. M. O., "Calculation of Viscous Drag and Turbulent Boundary-Layer Separation on Two-Dimensional and Axisymmetric Bodies in Incompressible Flows," Rept. MDC J0973-01, 1970, Douglas Aircraft Co., Long Beach, Calif.

[4]Parsons, J. S. and Goodson, R. E., "The Optimum Shaping of Axisymmetric Bodies for Minimum Drag in Incompressible Flow," Rept. ACC-72-5, 1972, Automatic Control Center, School of Mechanical Engineering, Purdue University, West Lafayette, Ind.

[5]Patel, V. C., "On the Equations of a Thick Axisymmetric Turbulent Boundary Layer," Rept. 143, 1973, Iowa Institute of Hydraulic Research, Iowa City, Iowa.

[6]Patel, V. C., "A Simple Integral Method for the Calculation of Thick Axisymmetric Turbulent Boundary Layers," *The Aeronautical Quarterly*, Vol. 25, 1974, pp. 47–58.

[7]Landweber, L., "Potential Flow About Bodies of Revolution and Symmetric Two-Dimensional Flows," BuShips Index NS 715-102, 1959, Iowa Institute of Hydraulic Research, Iowa City, Iowa.

[8]Cornish, J. J. and Boatwright, D. W., "Application of Full Scale Boundary Layer Measurements to Drag Reduction of Airships," Rept. 28, 1960, Aerophysics Dept., Mississippi State University, State College, Miss.

[9]Lyon, H. M., "Flow in the Boundary Layer of Streamline Bodies," R & M 1922, 1934, British Aeronautical Research Council, London, England.

[10]Thwaites, B., "Approximate Calculation of the Laminar Boundary Layer," *Aeronautical Quarterly,* Vol. 1, 1949, pp. 245–280.

[11]Rott, N. and Crabtree, L. F., "Simplified Laminar Boundary-Layer Calculations for Bodies of Revolution and for Yawed Wings," *Journal of the Aeronautical Sciences,* Vol. 19, No. 8, Aug. 1952, pp. 553–565.

[12]Michel, R., "Etude de la Transition sur les Profiles d'aile; Establissement d'un Critere de Determination du Point de Transition et Calcul de la Trainee de Profile Incompresible," Rept. 1/1578A, 1951, ONERA Chatillon, France.

[13]Crabtree, L. F., "Prediction of Transition in the Boundary Layer on Aerofoil," *Journal of the Aeronautical Sciences,* Vol. 62, July 1958, pp. 525–528.

[14]van Ingen, J. L., "A Suggested Semi-Empirical Method for the Calculation of the Boundary Layer Transition Region," Rept. VTH 74, 1956, Delft, The Netherlands.

[15]van Driest, E. R. and Blumer, C. B., "Boundary-Layer Transition: Freestream Turbulence and Pressure Gradient Effects," *AIAA Journal,* Vol. 1, No. 6, June 1963, pp. 1303–1306.

[16]Jaffe, N. A., Okamura, T. T., and Smith, A. M. O., "Determination of Spatial Amplification Factors and their Application to Predicting Transition," *AIAA Journal,* Vol. 8, No. 2, Feb. 1970, pp. 301–308.

[17]Hall, D. J. and Gibbings, J. C., "Influence of Stream Turbulence and Pressure Gradient upon Boundary Layer Transition," *Journal of Mechanical Engineering Science,* Vol. 14, No. 2, 1972, pp. 134–146.

[18]Nash, J. F., "Turbulent Boundary-Layer Behaviour and the Auxiliary Equation," CP 835, 1965, Aeronautical Research Council, London, England.

[19] Thompson, B. G. J., "A New Two-Parameter Family of Mean Velocity Profiles for Incompressible Turbulent Boundary Layers on Smooth Walls," R & M 3463, 1965, Aeronautical Research Council, London, England.

[20]Head, M. R., "Entrainment in the Turbulent Boundary Layer," R & M 3152, 1958, Aeronautical Research Council, London, England.

[21]Shanebrook, J. R. and Sumner, W., "Entrainment Theory for Axisymmetric Turbulent Incompressible Boundary Layers," *Journal of Hydronautics,* Vol. 4, No. 4, Oct. 1970, pp. 159–160.

[22]Young, A. D., "The Calculation of the Total and Skin Fric-

tion Drags of Bodies of Revolution at Zero Incidence," R & M 1874, 1939, Aeronautical Research Council, London, England.

[23]Gertler, M., "Resistance Experiments on a Systematic Series of Streamlined Bodies of Revolution—For Application to the Design of High-Speed Submarines," Rept. C-849, 1950, David Taylor Model Basin, Naval Ship Research & Development Center, Washington, D.C.

[24]Freeman, H. B., "Measurements of Flow in the Boundary Layer of a 1/40-Scale Model of the U.S. Airship Akron," TR 430, 1932, NACA.

[25]Freeman, H. B., "Force Measurements on a 1/40-Scale Model of the U.S. Airship Akron," TR 432, 1932, NACA.

[26]Landweber, L. and Gertler, M., "Mathematical Formulation of Bodies of Revolution," Rept. 719, 1950, David Taylor Model Basin, Naval Ship Research and Development Center, Washington, D.C.